Building Tomorrow's Society

Bâtir la Société de Demain

Fredericton, Canada

June 13 – June 16, 2018/ *Juin 13 – Juin 16, 2018*

COMPARISON OF DIFFERENT ACCELERATED CORROSION TECHNIQUES

Said, Mahmoud. E[1,3], Hussein, Amgad[1], Hassan, Assem A[1] and Gillis, Nick.[2]
[1] Civil Engineering Department, Memorial University, Canada
[2] SNC Lavalin Inc, Canada
[3] meaeaas2@mun.ca

Abstract: This paper presents different techniques that could be used in conducting an accelerated corrosion experiments in a lab environment. The objective of the techniques is to induce corrosion in full-scale structural reinforced concrete members. The study aims to demonstrate the benefits and drawbacks of each technique. Two full scale reinforced concrete two-way slabs were prepared for this experiment. The slabs had an identical dimension of 1900 mm × 1900 mm × 150 mm. The slabs reached the same level of corrosion, 25% mass loss, using two different accelerated methods: constant voltage and constant current. The induced corrosion in each slab was evaluated. The corrosion state was examined based on current measurement, half-cell potential tests, and mass loss. Both techniques showed a close agreement between the actual mass loss and the theoretical mass loss that was calculated using Faraday's equation. During corrosion, the concrete loses its resistivity which is directly reflected by an increase in the current in the case of constant voltage. Hence, using constant voltage could cause damage more than that by normal environmental conditions. Whereas constant current technique keeps the current intensity uniform over the corrosion process regardless of the resistivity of concrete, leading to uniform corrosion rate which avoid extreme damage.
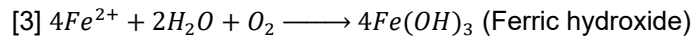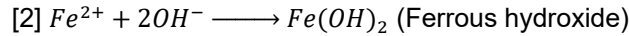
Keywords: Accelerated corrosion, Constant voltage, Constant current, Two-way Slabs

1   INTRODUCTION

The corrosion of reinforced concrete (RC) elements occurs due to the difference in the electrical potential along the reinforcement. This process is considered as an electrochemical process, where an anode is created at a certain part of the bar. At the anode, electrons are released due to an oxidation reaction. Whereas a cathode part is created by attracting the released electrons due to the reduction reaction that occurs at certain another part of the bar. The released electrons flow through an electrolyte solution from the anodic side to the cathodic side. In the cathodic part, the negative electrons convert to hydroxyl ions (OH^-) (oxidizing agent) in the presence of moisture and oxygen as:

$$[1] \quad O_2 + 2H_2O + 4e^- \longrightarrow 4\,OH^-$$
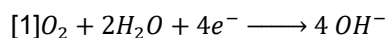
These hydroxyl ions travel through the electrolyte solution (concrete pore water) and combine with the ferrous ions to form iron hydroxides($Fe(OH)_2$). In the presence of oxygen and moisture, the ferrous hydroxide ($2Fe(OH)_2$) converts to ferric oxide ($Fe_2O_3H_2O$), i.e. rust (Neville, 2011).

[2] $Fe^{2+} + 2OH^- \longrightarrow Fe(OH)_2$ (Ferrous hydroxide)

[3] $4Fe^{2+} + 2H_2O + O_2 \longrightarrow 4Fe(OH)_3$ (Ferric hydroxide)

It is concluded that corrosion needs three elements to exist: a chemical potential difference between the two sides of the steel bar; an electrolyte solution to provide conductivity; and an electron path through the metal to allow the flow of electrons (Neville, 2011). This corrosion mechanism is similar to flashlight battery mechanism. Therefore, accelerated corrosion techniques innovated from the idea of flashlight battery in order to simulate corrosion inside a lab under normal environmental conditions (Amleh, 2000).

The corrosion process naturally needs a long period to occur. Therefore, researchers use accelerated corrosion techniques to speed up the corrosion process to save time and money. Accelerated corrosion tests are used to investigate the behavior of corroded structural elements. The objective of such research is to correlate the accelerated corroded laboratory results and the real corrosion that occurs to existing structures (Davis, 2000). The mass loss due to corrosion is controlled using a direct electrical current, in which Faraday's equation is used to predict the mass loss (Toongoenthong and Maekawa, 2004). Current is applied through the application of constant voltage or constant current. There are several studies in the literature that used constant voltage (Amleh, 2000; Lee *et al.*, 2000; Ahwazi, 2001; Kumar *et al.*, 2012; Deb and Pradhan, 2013; Pellegrini-Cervantes *et al.*, 2013; Al-Swaidani and Aliyan, 2015), and others used constant (impressed) current (El Maaddawy and Soudki, 2003; El Maaddawy, Soudki and Topper, 2005; Kashani, Crewe and Alexander, 2013; Pritzl, Tabatabai and Ghorbanpoor, 2014; Talakokula, Bhalla and Gupta, 2014; Altoubat, Maalej and Shaikh, 2016). Generally, in both techniques, an electrochemical potential is created between the embedded reinforcement inside the concrete that acts as an anode and copper or steel mesh as a cathode. The cathode could be external or internal (embedded inside concrete). An electrolyte solution such as chloride salts solution is used to activate the corrosion process (El Maaddawy and Soudki, 2003).

In constant current technique, an electrical power supply provides constant current densities through the specimen to reach a certain level of corrosion (El Maaddawy and Soudki, 2003). In contrast, the constant voltage technique adjusts the power supply through the application of constant volt. The constant volt in several studies varied from 5V to 30V (Ahwazi, 2001; Yoon *et al.*, 2001; Xia, Jin and Li, 2012). The corrosion is monitored by measuring the current using a computer-controlled data acquisition system.

Altoubat et al. (2016) conducted an experimental study that illustrated the effect of both accelerated corrosion techniques (constant voltage and constant current) on the corrosion behavior of small-scale columns. They noticed that the damage created in the specimen by constant current is more than that by constant voltage. Nonetheless, both techniques caused the same mass loss in the corroded reinforcement. The authors recommended the use of constant current technique to simulate corrosion damage, especially it ensures that the targeted corrosion level is reached within a reasonable amount of time.

Several studies used the impressed current techniques with different current densities that ranged from $45 \mu A / cm^2$ as a minimum value to $10400 \mu A / cm^2$ as a maximum value (Almusallam *et al.*, 1996; Bonacci *et al.*, 1998). El Maaddawy & Soudki (2003) concluded that the variation in current densities has no effect on the percentage of mass loss that was calculated based on Faraday's law. Their specimens reached mass loss up to 7.27%. However, they noticed that using current density above $200 \mu A / cm^2$ would cause a significant increase in crack width and strain response due to the corrosion. The authors also recommended not to use different current densities for to reach different levels of corrosion. It was concluded that changing the current densities to obtain different levels of corrosion may misguide the analysis of test results.

To the best of the authors' knowledge, the literature only covers accelerated corrosion techniques that have been used to induce corrosion in RC beams, but there are no previous studies that have been carried out on two-way slabs using any such techniques. This could be attributed to the challenges that could face researchers to induce corrosion in two-way slabs. The number of corroded bars in two-way slabs are more than those in beam or one-way slabs. Therefore, a corrosion experiment of two-way slabs needs data acquisition systems with large number of free channels to record the current readings and requires long

period of time. Lab-space availability for a longer period of time could be a challenge. Furthermore, the reinforcement of any two-way slab consists of two meshes (flexural and compression) and each mesh consists of two layers. It requires special attention to isolate each rebar to ensure uniform corrosion. This paper aims to demonstrate a lab setup that could be used to induce corrosion in two-way slab using constant current or constant voltage. The advantage and disadvantage of using each technique will be demonstrated. The authors believe that this study will provide some knowledge to guide the future researchers to choose the suitable accelerated approach to investigate the effect of corrosion on full-scale RC two-way slabs.

## 2   EXPERIMENTAL PROGRAM

2.1   Details of Test Specimens

Two RC slabs with the same identical dimension and reinforcement were cast. Each slab had dimensions of 1900 × 1900 × 150 mm with clear cover of 30 mm and 1% flexural reinforcement distributed uniformly using 15M bars that are spaced at 190 mm as shown in Figure 1. The details of the test specimens are shown in Table 1. The reinforcement was weighted before casting to enable the calculation of the mass loss after the corrosion test. All intersection points between bars were carefully isolated to control and ensure uniform corrosion in each corroded bar. An electrical wire was connected at the end of the tested bars from both ends.
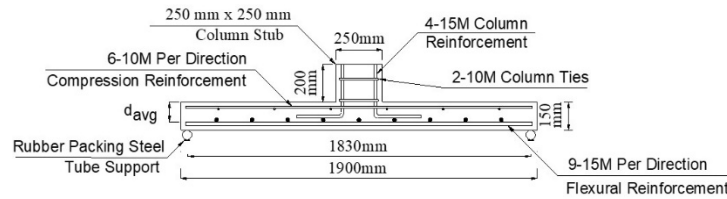
Table 1 Details of Test Slabs

Side dimensions (mm × mm)	h (mm)	c (mm)	d (mm)	f_c' (MPa)	Main reinforcement
1900 × 1900	150	250	104	41.1	Two layers of 15M bars (ρ = 1%)

*h is the height; c is column width; d is the effective slab depth; ρ is the reinforcement ratio; and f_c' is the concrete compressive strength.
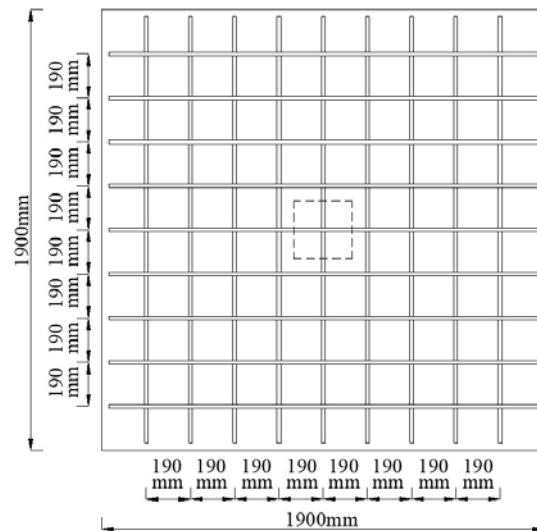

a. Flexural mat reinforcement 15M @ 190 mm

b. Cross-section of the slab

Figure 1: Details of a typical slab

Figure 2 shows a slab specimen and the form work used. Two slabs were under investigation on this study. The first slab (SV) was corroded till reach 25% mass loss using constant voltage accelerated corrosion technique. The second slab (SC) reached the same level of corrosion but by using constant current accelerated corrosion technique.
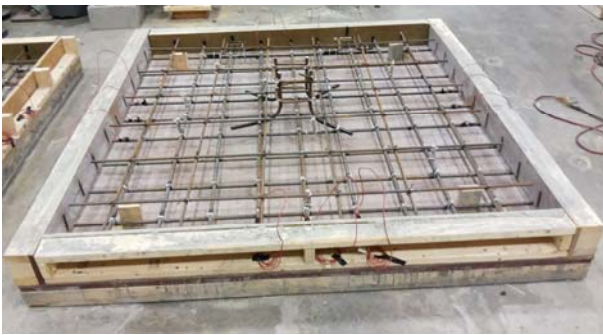
(a)
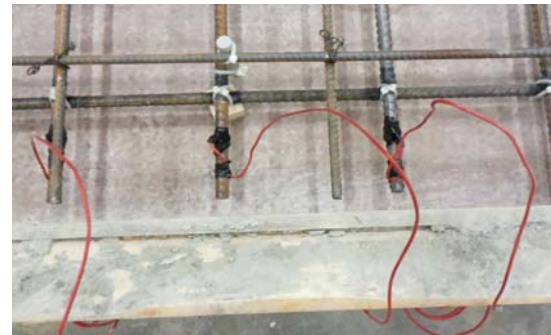
(b)

Figure 2: Test specimens: (a) reinforcement mesh; (b) wire-bar connection

2.2   Material Properties

Table 2 shows the concrete mixture composition used in casting the slabs. Based on the recommendation of ACI 318-14 concrete horizontal elements exposed to de-icing salts are classified as class F3. Under such exposure, the targeted concrete strength has to be at least 40 MPa and the w/c ratio should not be more than 0.4 (ACI Committe-318, 2014). Table 3 shows the actual properties of the concrete and the reinforcement.

Table 2 Mixture Composition of Concrete Mix

Cement (kg)	Water/cement ratio	Water (L)	Coarse/fine ratio	Coarse aggregate (kg)	Fine aggregate (kg)	Aggregate size (mm)	Fresh density (kg/m3)
350	0.4	140	1.3	1083	833	10	2407

Table 3 Steel and Concrete Properties

	Steel properties			Concrete Properties	
Designation	Area mm^2	f_y MPa	ε_y ($\mu\varepsilon$)	f_c' MPa	f_r MPa
15M	200	475	2200	41.1	3.82

Ready mix concrete was used based on specific mix design. Before casting, the slump was measured, and the prisms and cylinders were prepared. The poured concrete was consolidated using an electrical vibrator. The column stub was cast on the next day. The form work was removed after 24 hrs from casting the column stub. Water curing process continued for four days followed by air curing for 28 days.

2.3 Accelerated Corrosion Setup

After casting the slabs, each slab was placed upside down in leveled position. A dike wall tank was built over the targeted corrosion area using foam sheets. The dike was connected to a hose with a valve to facilitate the drainage of the dike from the electrolyte solution when needed. The hose was located at the lower level point of the dike. A steel mesh was placed inside the dike to act as a cathode. The tank was filled with a chloride salt solution with concentration of 5% by weight of the water. A power supply was used to provide a direct current by connecting the positive charge to the tension reinforcement and the negative charge to the steel mesh. The direct current connected to slab SV through the application of constant voltage and connected to slab SC through the application of constant current. The theoretical mass loss is calculated based on Faraday's equation as shown in Eq. (4):

$$[4] \quad \text{Mass loss} = \frac{t\, i\, M}{z\, F}$$

Where t is the time passed in seconds, i is the current passed in amperes, M is atomic weight (for iron $M = 55.847$ g/mol), z is the ion charge (two moles of electrons) and F is Faraday's constant which is the amount of electrical charge in one mole of electron ($F = 96,487$) (Lachemi *et al.*, 2014).

2.3.1 Constant Voltage Technique Setup

The Constant voltage accelerated corrosion setup consisted of: power supply, data acquisition systems, current transducers, distribution board, electrolyte solution, steel mesh, and computer to process the data. Figure 3 shows the elements used in the setup.

Computer-controlled data acquisition system
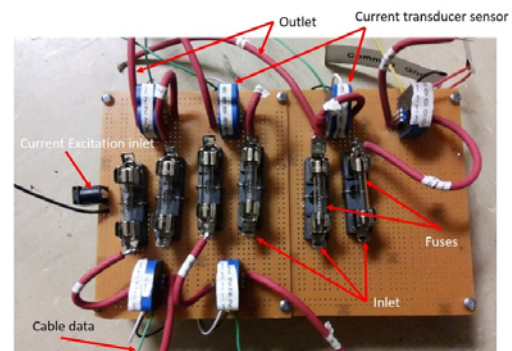
Current transducer board

Figure 3: Constant voltage accelerated test setup

A power supply was adjusted to provide a constant voltage 15 V. The positive terminal was connected to distribution board that distributed the input current into several output terminals with the same constant voltage 15 V, as a parallel circuit. The data acquisition system read the voltage value. On the other hand, the current value was needed to calculate the mass loss according to Faraday's equation. Hence, special current transducers were used to convert the current reading to voltage. Accordingly, each output terminal was connected to a current transducer. The output of the current transducers was recorded using the data acquisition system and stored in a computer. The outlet from each transducer in the current transducer board was connected to the bars under corrosion process. The negative terminal from the power supply was connected directly to the steel mesh that served as a cathode. The steel mesh was immersed inside the electrolyte solution inside the dike above the corroded targeted area.

2.3.2 Constant Current Technique Setup

Constant current accelerated corrosion setup consisted of: power supply, electrolyte solution, and steel mesh. Figure 4 shows the elements used in the setup for constant current technique. Each corroded bar needed a separate power supply in order to control the mass loss and to ensure uniform corrosion in all corroded bars. Each power supply was adjusted to apply current density of $200\,\mu A/cm^2$. This value was chosen according to the recommendations of El Maaddawy & Soudki (2003) that the current density should not exceed $200\,\mu A/cm^2$ to avoid any significant increase in crack width and strain response due to the corrosion. The counting of corrosion time started after the half-cell potential read more than -350 mV to ensure that the current overcome the concrete resistant and the occurrence possibility of corrosion was more than 90% (ASTM C876, 2015).

Figure 4: Constant current accelerated corrosion technique setup

3 EXPERIMENTAL RESULTS AND ANALYSIS

3.1 Time-dependent corrosion tests results

3.1.1 Current Results

Slab SC was corroded under the application of constant current. The current intensity applied was $200\,\mu A/cm^2$ which was equivalent to 0.1 A. This current was applied for 146 days until the targeted corrosion level of 25% mass loss was reached. This technique enable the determination of the exact time. On the other hand, slab SV was corroded under the application of constant voltage 15 V. The current was monitored using a computer-controlled data acquisition system. Figure 5 shows the relation between the current and the elapsed time for a corroded bar. It could be noticed that the current initially slightly dropped down then remained constant for almost 84 days. This was followed by a linear increase till the targeted

level of 25% of mass loss was reached. The slight drop down in the current could be ascribed to the presence of the passive film layer around the bar that prevented it against corrosion. Then, the current weakened this layer with the help of chloride ingress, the corrosion started and its rate increased progressively. The sudden jump in the current could be attributed to the bond loss between the corroded bar and the concrete cover in which spalling of concrete covers started to occur.

Figure 6 shows the mass loss rate versus time for a corroded bar. It can be seen that the mass loss rate increased with increasing the current rate, which is associated with increasing the rate of corrosion. At the end of corrosion process, the current intensity exceeded $200 \mu A / cm^2$, which surpassed the recommended from El Maaddawy & Soudki (2003). This would cause a significant increase in crack width due to the corrosion.
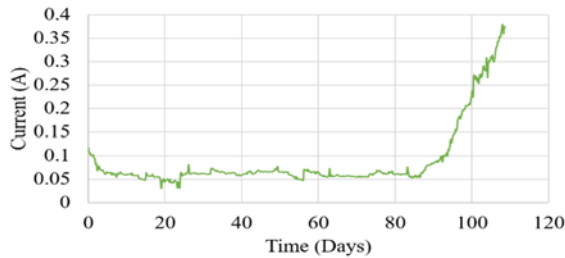
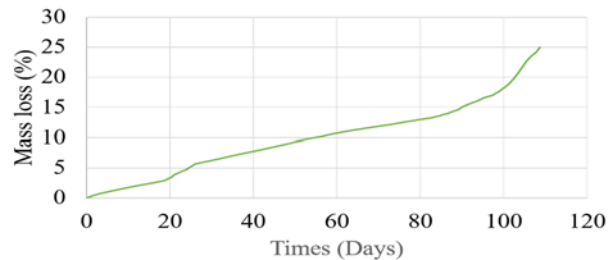Figure 5: Current time history for SV specimen   Figure 6: Mass loss rate with time

3.1.2   Half-Cell Potential Measurements

The half-cell potential readings are an indication of the existence of corrosion. Higher probability of existing corrosion is expected when the reading of the half-cell potential gives more negative values. The half-cell potential was used to determine the corrosion of the reinforcement in accordance with (ASTM C876, 2015).

The half-cell potential was used on slab SC at the beginning of the test. It was used to determine the instance of the occurrence of corrosion to count the time lapsed in order to calculate the mass loss based on Faraday's equation. The corrosion time started when the half-cell read -350 mV. The half-cell potential was used to evaluate the corrosion process for slab SV during the entire experiment. The half-cell readings were recoded once every three days at twenty-four different location that cover the entire corroded area. Figure 7 shows the half-cell reading versus time over the corroded area. The potential reading was measured directly above the flexural reinforcement mesh. The mesh consisted of two layers; top and lower ones. Figure 8 shows the reading variation of half-cell versus the level of corrosion. It can be seen from both figures that the corroded bars in the upper layer had more negative values than the lower one. This could be attributed to the concrete cover for the upper layer that was smaller than upper one by 16 mm. Hence, the upper layer was exposed to more chlorides ingress than the lower one. This result is in good agreement with previous studies that the concrete cover has a significant effect on the half-cell potential values (Klinghoffer, 1995). It can be also noticed from both figures that there was no variation in the reading of the half-cell when the corrosion started. Therefore, this test was used only as an indication of the occurrence probability of corrosion for un-corroded members.
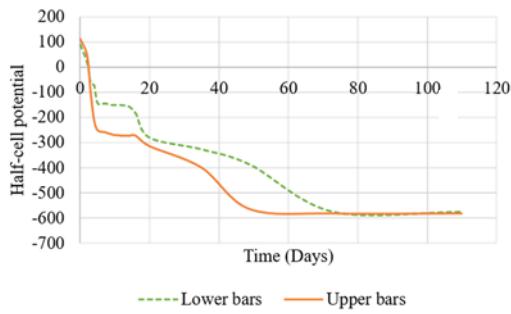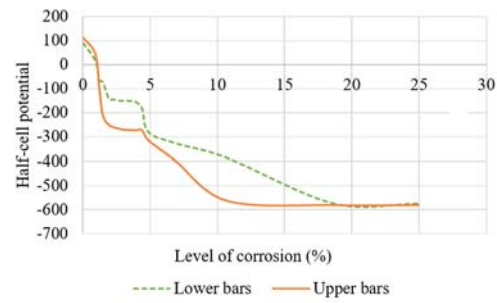
Figure 7: Half-cell potential reading vs. time   Figure 8: Half-cell potential readings vs. corrosion level

3.2 Test Results after Corrosion

3.2.1 Mass Loss

After the loading test was completed, the concrete cover was removed and the corroded bars were extracted from the slabs. The corrosion products were removed from the bars using a wire brush, then the bars were soaked in a HCL solution according to ASTM Standards G1-03 method (ASTM G1, 2003). Next, the bars were brushed again lightly to remove the remaining loose corrosion products. The cleaned bars were weighted and each bar was compared with its original weight. The reinforcement were weighed and labeled before casting and pouring the concrete. The percentage mass loss for each bar was calculated based on Eq. (5):

$$[5]\quad \% \text{ mass loss} = \frac{\left(\text{initial weight - final weight}\right)}{\text{initial weight}}$$

The actual mass loss for both slabs showed a close agreement with the theoretical mass loss. It was noticed that the actual mass loss was less than the theoretical ones for both slabs. This could be ascribed to the loss in current through concrete cover to overcome the concrete resistivity. Thus, this amount of current did not contribute to reducing the reinforcement mass due to corrosion. This conclusion was reached by several researchers (Auyeung, Balaguru and Chung, 2000; Spainhour and Wootton, 2008). However, the Faraday's equation gives a close agreement between actual and predicted mass loss regardless to the accelerated corrosion technique used. Figure 9 shows the corrode reinforcement for both slabs after removing the concrete cover.

a. Slab SV   b. Slab SC

Figure 9: Extracted corroded bars

4   CONCLUSIONS

In this paper, a lab setup that could be used to induce corrosion in two-way slabs was presented. Two techniques, constant current and constant voltage were used. The following conclusions were reached:

- Constant current technique could be more feasible than constant voltage technique. Most labs are equipped with data acquisition systems that read voltage. Each corroded bar using constant voltage technique will need an individual current transducer to convert it to voltage and a free channel in the data acquisition system. When using constant current, a power supply has to be provided for each. The combined cost of current transducers and data acquisition system could be more expensive than simple power supplies that are used in constant current technique.
- The constant voltage produces large volume of raw data that are needed to be processed every day to calculate the mass loss. Moreover, the data needs to be continuously stored and monitored to avoid any corruption of the file due to the accumulated recorded data.
- In constant current, the time period required for corrosion could be easily estimated before the test. Constant voltage does not have this option as the current changes with time. The constant voltage technique for high levels of corrosion could take less time than constant current because the current could reach very high values, although surge in current values should not be recommended in this type of testing.
- The current can reach very high values in constant voltage technique, which could exceed the recommended value of $200 \mu A / cm^2$ according to El Maaddawy & Soudki (2003). This increase could cause an increase in the concrete crack width leading to more damage than that caused by real corrosion.
- The concrete resistance increases with time; therefore, high voltage would be needed to overcome this resistance. Subsequently, the corrosion test for constant voltage should not be used with aged concrete. Rather, it would be recommended to start the test directly after 28 days from casting the concrete to avoid any possible increase that could happen in concrete resistance. Using constant current could be a better option to use with aged concrete since the required voltage also increases while keeping the current constant.

Accordingly, the authors believe that using constant current could be a better option when it comes to available lab facilities, space and time. Moreover, for severe levels of corrosion, constant current could better simulate the performance of real corroded elements compared to constant voltage.

References

ACI Committe-318 (2014) Building code requirement for structural concrete (ACI 318M-14) and commentary (ACI 318RM-14), Building Code Requirements for Structural Concrete.

Ahwazi, B. B. N. (2001) A comparative study of deterioration of bond due to corrosion in different concretes. McGill University.

Al-Swaidani, A. M. and Aliyan, S. D. (2015) 'Effect of adding scoria as cement replacement on durability-related properties', International Journal of Concrete Structures and Materials. Korea Concrete Institute, 9(2), pp. 241–254. doi: 10.1007/s40069-015-0101-z.

Almusallam, A., Al-Gahtani, A. S., Aziz, A. R. and Rasheeduzzafar, A. (1996) 'Effects of reinforcement corrosion on bond strength', Construction and Building Materials, 10(2), pp. 123–129.

Altoubat, S., Maalej, M. and Shaikh, F. U. A. (2016) 'Laboratory simulation of corrosion damage in reinforced concrete', International Journal of Concrete Structures and Materials. Korea Concrete Institute, 10(3), pp. 383–391. doi: 10.1007/s40069-016-0138-7.

Amleh, L. (2000) Bond deterioration of reinforcing steel in concrete due to corrosion. McGill University.

ASTM C876 (2015) Standard test method for corrosion potentials of uncoated reinforcing steel in concrete. doi: 10.1520/C0876-09.2.

ASTM G1 (2003) Standard practice for preparing, cleaning, and evaluation corrosion test specimens.

Auyeung, Y., Balaguru, P. and Chung, L. (2000) 'Bond behavior of corroded reinforcement bars', Materials Journal, 97(2), pp. 214–220.

Bonacci, J., Thomas, M., Hearn, N., Lee, C. and Maalej, M. (1998) 'Laboratory simulation of corrosion in reinforced concrete and repair with CFRP wraps', in Annual Conference of the Canadian Society of Civil Engineering, pp. 653–662.

Davis, J. (2000) Corrosion: understanding the basics. doi: 10.1361/cutb2000p001.

Deb, S. and Pradhan, B. (2013) 'A study on corrosion performance of steel in concrete under accelerated condition', in Proceedings of the International Conference on Structural Engineering Construction and Management, Kandy, Sri Lanka. Available at: http://dl.lib.mrt.ac.lk/handle/123/9365.

Kashani, M. M., Crewe, A. J. and Alexander, N. A. (2013) 'Nonlinear stress-strain behaviour of corrosion-damaged reinforcing bars including inelastic buckling', Engineering Structures, 48, pp. 417–429. doi: 10.1016/j.engstruct.2012.09.034.

Klinghoffer, O. (1995) 'In situ monitoring of reinforcement corrosion by means of electrochemical methods', Nordic Concrete Research, 95(1), pp. 1–13. Available at: http://www.germann.org/Publications/GalvaPulse/2. Klinghofer, O., In Situ Monitoring of Reinforcement Corrosion by means of Electrochemical Methods, Nordic Concrete Research 95 1.pdf.

Kumar, M. K., Rao, P. S., Swamy, B. L. P. and Chandra Mouli, C. (2012) 'Corrosion resistance performance of fly ash blended cement concrete', Internatioanl Journal of Research in Engineering and Technologi, 1(3), pp. 448–454. doi: 10.1016/0140-6701(95)93047-7.

Lachemi, M., Al-Bayati, N., Sahmaran, M. and Anil, O. (2014) 'The effect of corrosion on shear behavior of reinforced self-consolidating concrete beams', Engineering Structures. Elsevier Ltd, 79, pp. 1–12. doi: 10.1016/j.engstruct.2014.07.044.

Lee, C., Bonacci, J. F., Thomas, M. D. a., Maalej, M., Khajehpour, S., Hearn, N., Pantazopoulou, S. and Sheikh, S. (2000) 'Accelerated corrosion and repair of reinforced concrete columns using carbon fibre reinforced polymer sheets', Canadian Journal of Civil Engineering, 27(5), pp. 941–948. doi: 10.1139/cjce-27-5-941.

El Maaddawy, T. A. and Soudki, K. A. (2003) 'Effectiveness of impressed current technique to simulate corrosion of steel reinforcement in concrete', Journal of Materials in Civil Engineering. American Society of Civil Engineers, 15(1), pp. 41–47.

El Maaddawy, T., Soudki, K. and Topper, T. (2005) 'Analytical model to predict nonlinear flexural behavior of corroded reinforced concrete beams', ACI Structural Journal, 102(No. 4), pp. 550–559.

Neville, A. M. (2011) Properties of concrete (Fifth Edition), Cement and Concrete Research. doi: 10.1016/0008-8846(96)82366-0.

Pellegrini-Cervantes, M. J., Almeraya-Calderon, F., Borunda-Terrazas, A., Bautista-Margulis, R. G., Chacón-Nava, J. G., Fajardo-San-Miguel, G., Almaral-Sanchez, J. L., Barrios-Durstewitz, C. P. and Martinez-Villafañe, A. (2013) 'Corrosion resistance, porosity and strength of blended portland cement mortar containing rice husk ash and nano-SiO2', International Journal of Electrochemical Science, 8(8), pp. 10697–10710.

Pritzl, M. D., Tabatabai, H. and Ghorbanpoor, A. (2014) 'Laboratory evaluation of select methods of corrosion prevention in reinforced concrete bridges', International Journal of Concrete Structures and Materials, 8(3), pp. 201–212. doi: 10.1007/s40069-014-0074-3.

Spainhour, L. K. and Wootton, I. A. (2008) 'Corrosion process and abatement in reinforced concrete wrapped by fiber reinforced polymer', Cement and Concrete Composites. Elsevier, 30(6), pp. 535–543.

Talakokula, V., Bhalla, S. and Gupta, A. (2014) 'Corrosion assessment of reinforced concrete structures based on equivalent structural parameters using electro-mechanical impedance technique', Journal of Intelligent Material Systems and Structures, 0(0), pp. 1–16. doi: 10.1177/1045389X13498317.

Toongoenthong, K. and Maekawa, K. (2004) 'Interaction of pre-induced damages along main reinforcement and diagonal shear in RC members', Journal of Advanced Concrete Technology, 2(3), pp. 431–443. doi: 10.3151/jact.2.431.

Xia, J., Jin, W.-L. and Li, L.-Y. (2012) 'Effect of chloride-induced reinforcing steel corrosion on the flexural strength of reinforced concrete beams', Magazine of Concrete Research. Thomas Telford, 64(6), pp. 471–485.

Yoon, S., Wang, K., Weiss, W. and Shah, S. (2001) 'Interaction of reinforced between loading, corrosion, and serviceability of reinforced concrete', ACI Materials Journal, 97(6), pp. 637–644.